

# HarmonRank: Ranking-aligned Multi-objective Ensemble for Live-streaming E-commerce Recommendation

Boyang Xia  
xiaboyang.tech@gmail.com  
Kuaishou Technology  
Beijing, China

Hanxiao Sun  
sunhanxiao03@kuaishou.com  
Kuaishou Technology  
Beijing, China

Runnan Liu  
liurunnan@kuaishou.com  
Kuaishou Technology  
Beijing, China

Zhou Yu  
yuzhou03@kuaishou.com  
Kuaishou Technology  
Beijing, China

Biyun Han  
hanbiyun@kuaishou.com  
Kuaishou Technology  
Beijing, China

Zhiliang Zhu  
zhuzhiliang@zuaa.zju.edu.cn  
Unaffiliated  
Beijing, China

Jun Wang  
wangjun03@kuaishou.com  
Kuaishou Technology  
Beijing, China

Wenwu Ou  
ouwenwu@gmail.com  
Kuaishou Technology  
Beijing, China

## Abstract

Recommendation for live-streaming e-commerce is gaining increasing attention due to the explosive growth of the live streaming economy. Different from traditional e-commerce, live-streaming e-commerce shifts the focus from products to streamers. This shift requires the ranking mechanism to balance both purchases (short-term value) and user-streamer interactions (long-term value), *e.g.*, follows and comments, for the ecology health of the platform. To trade off multiple objectives, a popular solution is to build an ensemble model to integrate multi-objective scores into a unified score. The ensemble model is usually supervised by multiple independent binary classification losses of all objectives. However, this paradigm suffers from two inherent limitations. First, the optimization direction of the binary classification task is misaligned with the ranking task (evaluated by AUC). Second, this paradigm overlooks the alignment between objectives, *e.g.*, comment and buy behaviors are partially dependent which can be revealed in labels correlations. The model can achieve better trade-offs if it learns the aligned parts of ranking abilities among different objectives.

To mitigate these limitations, we propose a novel multi-objective ensemble framework **HarmonRank** to fulfill both alignment to the ranking task and alignment among objectives. For alignment to ranking, we formulate ranking metric AUC as a rank-sum problem and utilize differentiable ranking techniques for ranking-oriented optimization. For inter-objective alignment, we change the original *one-step* ensemble paradigm to a *two-step* one. In 1st step, we align each objective with other objectives in a self-attention mechanism.

In 2nd step, we fuse aligned objective encodings into the ensemble score with the guidance of personalized features.

Extensive offline experiments results on two industrial datasets and online experiments demonstrate that our approach significantly outperforms existing state-of-the-art methods. The proposed method has been fully deployed in Kuaishou's live-streaming e-commerce recommendation platform with 400 million DAUs, contributing over 2% purchase gain.

## CCS Concepts

- Information systems → Recommender systems..

## Keywords

Multi-objective ranking ensemble, Personalized recommendation, Learning to rank

## ACM Reference Format:

Boyang Xia, Zhou Yu, Zhiliang Zhu, Hanxiao Sun, Biyun Han, Jun Wang, Runnan Liu, and Wenwu Ou. 2026. HarmonRank: Ranking-aligned Multi-objective Ensemble for Live-streaming E-commerce Recommendation. In . ACM, New York, NY, USA, 10 pages. <https://doi.org/10.1145/nnnnnnn>.

## 1 Introduction

Live-streaming e-commerce market has recently experienced explosive growth. Different from traditional e-commerce, the products are endorsed and promoted by streamers in live-streaming e-commerce, which shifts the focus from products to the streamer. This paradigm shift necessitates a change from purchase-oriented ranking mechanism to multi-objective balanced mechanism including interactions between users and streamers, *e.g.*, follows and comments. Different from short-term purchase, these interaction-oriented objectives matter to the ecosystem for the their long-term value. For an example, *follow* behaviors can foster long-term user-streamer relationships, which helps to the ecology health of the platform. This change poses more challenges for balancing these

Permission to make digital or hard copies of all or part of this work for personal or classroom use is granted without fee provided that copies are not made or distributed for profit or commercial advantage and that copies bear this notice and the full citation on the first page. Copyrights for components of this work owned by others than the author(s) must be honored. Abstracting with credit is permitted. To copy otherwise, or republish, to post on servers or to redistribute to lists, requires prior specific permission and/or a fee. Request permissions from [permissions@acm.org](mailto:permissions@acm.org).

Conference'17, Washington, DC, USA

© 2026 Copyright held by the owner/author(s). Publication rights licensed to ACM. ACM ISBN 978-x-xxxx-xxxx-x/YYYY/MM  
<https://doi.org/10.1145/nnnnnnn.nnnnnnn>

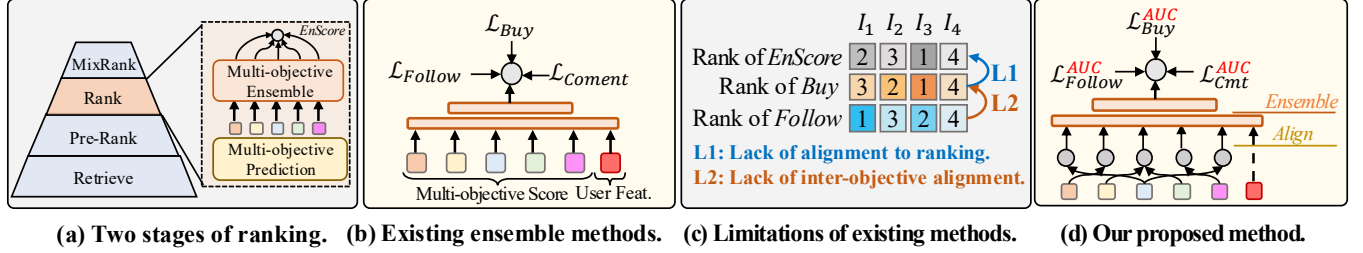


**Figure 1: Conceptual view of the multi-objective ensemble stage and different ensemble paradigms.** (a) The position of multi-objective ensemble stage in industrial recommender systems. (b) Existing one-step ensemble paradigm based on multi-layer non-linear with multiple binary classification losses. (c) Limitations of existing paradigm. First, lack of the alignment to ranking task. Second, lack of the alignment between objectives.(d) Our proposed paradigm to fulfill alignment to ranking and inter-objective alignments.

competing objectives than traditional purchase-driven e-commerce recommender systems.

To balance these competing objectives, industrial ranking systems usually follow a two-stage paradigm (see Fig. 1 (a)), *i.e.*, multi-objective prediction (MP) and multi-objective ensemble (ME) [3, 4, 11, 16]. The MP stage is usually a high-capacity multi-task learning model [13] whose goal is to predict the precise probability scores for multiple objectives, *e.g.*, click through rate (CTR). Whereas ME stage is a light-weight model whose goal is to generate a unified ensemble score in a personalized manner. It usually only takes aforementioned multi-objective scores and a few user features as inputs. The ensemble score is used to truncate top items to represent for users. In this paper, we focus on ME problem. Similar to MP stage, in ME stage we use AUC (Area Under ROC Curve) [1] between the ensemble score and the ground-truth labels to evaluate the ranking abilities of the ensemble model. The only difference is that we utilize the sum of AUC of all objectives as the metric for comprehensive multi-objective ranking evaluation.

The key challenge at this stage lies in the absence of a gold-standard supervision to comprehensively assess items considering multiple objectives. To mitigate this problem, a typical solution is to impose multiple independent binary classification supervisions over the ensemble score [3, 12] (see Fig. 1 (b)). However, this paradigm suffers from two limitations, for which we present a conceptual view in Fig. 1 (c). **(1) Lack of alignment to ranking task.** The optimization directions of binary classification based supervisions are misaligned with the ultimate ranking task (evaluated by AUC) [19]. For an example, if the positive labels of some action are highly sparse, a dummy predictor which predicts all instances as negative seems to present an acceptable binary classification result. But it actually yields a poor ranking results with an AUC of 0.5. **(2) Lack of inter-objective alignment.** The different objectives are neither independent nor strictly adversarial - they are partially dependent. For an example, *buy* actions empirically exhibit high correlations with *comment* actions, which can be verified through the statistical analysis of correlation between objectives (see Fig.4). Thus, if model can learn the aligned parts among multi-objectives, it is easier for model to trade-off these competing objectives.

To mitigate these issues, in this paper, we propose a novel personalized multi-objective ensemble framework **HarmonRank**, which enables both alignment to the ranking task and alignment between multiple objectives. For alignment to ranking, we firstly reformulate the non-differentiable AUC as a rank sum problem. Then we utilize an advanced differentiable ranking technique to optimize multi-objective AUC in an end-to-end manner. For alignment between objectives, we propose to change existing *one-step* ensemble architecture to a *two-step* one, *i.e.*, first *align* then *ensemble*. In *align* step, we align the common parts between multiple objectives via self-attention mechanism. In *ensemble* step, we fuse the aligned encodings of all objectives into ensemble score. In this process, we compress personalized information into a query and enable user-specific ensemble by cross attention mechanism.

Overall, our contributions can be summarized as follows:

- We propose a novel personalized multi-objective ensemble framework HarmonRank to enable the alignment of optimization to the ranking task with differentiable AUC optimization.
- We propose a *two-step* ensemble paradigm to enable align the shared parts between multiple objectives, to obtain better trade-off between objectives.
- We conduct extensive offline experiments on two industrial recommendation datasets. Experimental results demonstrate that our HarmonRank achieves superior performance over all existing state-of-the-art methods. Additionally, HarmonRank contributes more than 2% purchase gain for Kuaishou live-streaming e-commerce platform.

## 2 Related Work

### 2.1 Multi-objective optimization in recommender systems

Multi-objective optimization is recognized as a key challenge in both research and industry community. Early recommender systems primarily optimized for only few objectives, *e.g.* click-through rate (CTR) prediction for e-commerce recommender system and watch time for video recommender systems. However, with the

increasing complexity user interface functionalities, modern recommender system need to balance more competing objectives. Some studies attend on the sample selection bias caused by chain relationships between objectives, *e.g.*, CTR and conversion rate (CVR) [5, 14]. Some other researchers are dedicated to improve multi-task learning mechanism between different objectives [13, 18]. For an example, Multi-gate Mixture-of-Experts (MMOE) [13] architecture addresses this by leveraging expert networks to capture shared representations across objectives, thereby improving accuracy of individual objectives. Despite these advances, how to ensemble multiple prediction scores of different objectives remains a non-trivial challenge. Current industrial systems typically address this through a multi-objective ensemble model [11, 16, 22].

## 2.2 Multi-objective Ensemble in recommender systems

Early industrial approaches predominantly employed ranking formulas to combine scores from multiple objectives, typically optimizing parameters through grid search. While black-box optimization methods, *e.g.*, Bayesian optimization [15] and cross entropy methods [17], can reduce the iterations for searching optimum, they still suffer from two critical limitations: (1) inability to present personalized ranking mechanism to adapt user preferences, and (2) incapacity to exploit real-time user feedback. The factors matter for system since the optimal ensemble schemes change with different users and different time. To address these challenges, recent methods have proposed model-based ensemble solutions, to utilize more informative features and deep neural networks trained in hourly updated streaming feedback.

The key challenge for model-based multi-objective ensemble lies in the absence of a gold-standard supervision across multiple objectives. To solve this problem, some methods apply multiple unilateral binary classification losses to optimize towards all objectives simultaneously [3, 12], which can be referred as *loss aggregation* methods. The other methods aim to build a unified supervision by aggregating multiple binary labels into a single regression label [4, 11], which can be categorized as *label aggregation* methods. Despite these efforts, the optimization directions of these methods' supervisions are misaligned with the ultimate ranking task (evaluated by AUC), which leads to suboptimal performance. Reinforce learning based methods [16] can directly optimize towards ranking task metrics (AUC sum), whereas their policy gradients suffer from large variance and instability. Few of existing methods consider to optimize final sum of AUC in an end-to-end differentiable manner. It is NP-hard to direct optimize AUC because of the non-convexity and discontinuousness of [7].

## 2.3 AUC optimization

The AUC is a ranking quality metric defined based on pairwise comparisons [1, 9] under binary label settings. Thus, traditional differentiable AUC optimization methods concentrate on developing effective pairwise surrogate functions to approximate non-differentiable comparison function, *i.e.*,  $s_i - s_j \geq 0$ . For examples, pairwise square methods [6] employ square functions  $(1 - (s_i - s_j))^2$  surrogate functions, while pairwise logistic methods [7] propose to use logistic function  $\log(1 + \exp(-(s_i - s_j)))$  to approximate

the comparison function. However, the inherent  $O(n^2)$  time complexity of pairwise approaches renders them impractical for large-scale datasets. Consequently, numerous optimization attempts have shifted towards instance-wise AUC optimization. Leveraging the special form of pairwise square, pairwise AUC maximization can be decomposed into a min-max instance-wise formulation [21], with  $O(N)$  time complexity. Nevertheless, this instance-wise optimization introduces much sensitivity to noisy samples. To address this, AUCM [24] proposed a margin-based min-max optimization strategy to effectively mitigate this issue.

While recent advancements improve the computational complexity to  $O(N)$ , they inadvertently introduce greater inconsistency with factual AUC computation due to computation simplification for surrogate functions. In this paper, to balance computational efficiency and AUC computation consistency, we propose a novel AUC optimization method under a rank based formulation other than pairwise formulation. We formulate AUC computation as a rank-sum problem in the ordered score list and utilize differentiable ranking technique to solve this rank-sum problem. Our method presents  $O(n \log n)$  time complexity and superior AUC optimization accuracy for alignment with AUC theoretical computation.

## 3 Problem Formulation

### 3.1 Input and output

Let  $\mathcal{I}_{\text{cand}}(\mathbf{u}, \mathbf{c}) = \{I_i\}_i^N$  be a requested candidate set for the user  $\mathbf{u}$  and environment context  $\mathbf{c}$  (*e.g.*, time and app version). For each item  $I_i$ , multi-objective prediction (MP) model estimates  $M$  kind of interaction scores  $\mathbf{e}_i \in \mathbb{R}^{[M,1]}$ , *e.g.*, purchase, long view, like, follow, *etc.* Multi-objective ensemble (ME) model is responsible for integrating these scores into an ensemble score in a personalized way:

$$s_i = \mathcal{F}(\mathbf{e}_i, \mathbf{u}, \mathbf{c}; \theta) \quad (1)$$

Then top items are selected and displayed to users based on top-k truncation of the ensemble scores  $\mathcal{S} = \{s_i\}_i^N$ , where  $\mathcal{F}(\cdot; \theta)$  is a neural-network ensemble model parameterized by  $\theta$ .

$$\mathcal{I}_{\text{realshow}} = \text{TopK}(\mathcal{I}_{\text{cand}}, \mathcal{S}) \quad (2)$$

### 3.2 Train and evaluation

Similar to MP stage, we collect multiple behavior feedback labels in a fixed waiting window for each exposed sample in logs, and we use these labels to supervise the ensemble model training. Our goal is to achieve improved trade-offs across competing objectives. Due to the high cost of online AB metric evaluation, we typically evaluate the ME model's comprehensive ranking abilities on all objectives by the sum of AUC on a offline dataset  $\mathcal{D} = \{(\mathbf{x}_i, \mathbf{y}_i)\}_{i=1}^N$ . Here  $\mathbf{y}_i \in \{0, 1\}^{[M,1]}$  is the ground truth interaction labels for the  $i$ -th sample:

$$\mathcal{G}_m(\mathcal{D}) = \frac{\sum_{s_i \in \mathcal{D}_m^+, s_j \in \mathcal{D}_m^-} \mathbb{I}(s_i \geq s_j)}{|\mathcal{D}_m^+| \cdot |\mathcal{D}_m^-|} \quad (3)$$

$$\mathcal{G}(\mathcal{D}) = \sum_{m=1}^M \mathcal{G}_m(\mathcal{D}) \quad (4)$$

where  $\mathcal{D}_m^+$  and  $\mathcal{D}_m^-$  represent the positive and negative sample sets defined on the  $m$ -th objective, *e.g.*, the purchased items and unpurchased items. Existing methods primarily rely on classification or

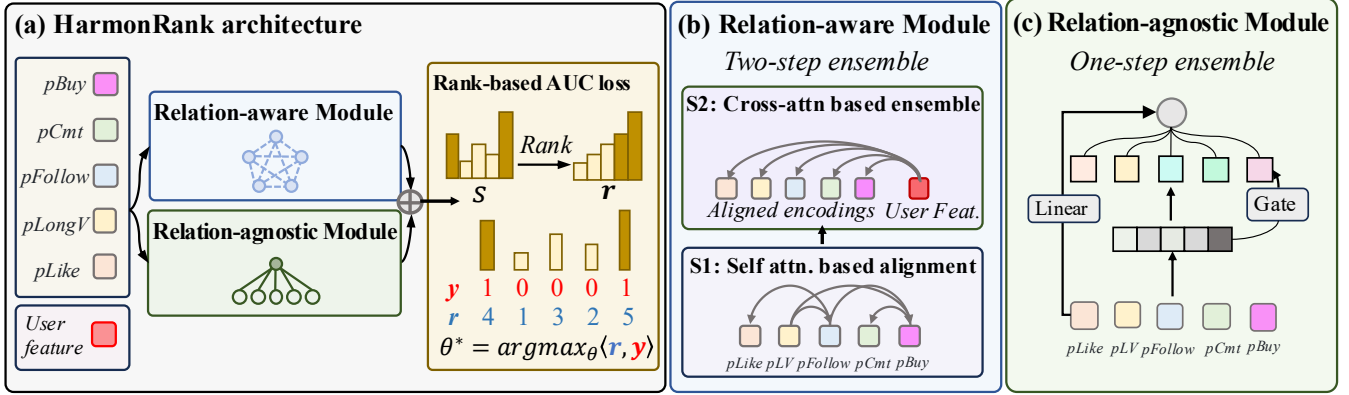


**Figure 2: Systematic overview of our HarmonRank framework.** (a) The architecture of HarmonRank. (b) Relation-aware module with inter-objective alignment and personalized guidance. (c) Relation-agnostic module with gate mechanism and linear fusion pathway. ‘pBuy’, ‘pCmt’, ‘pFollow’, ‘pLV’ and ‘pLike’ here represent the predicted probability scores corresponding to ‘buy’, ‘comment’, ‘follow’, ‘long view’ and ‘like’.

regression losses to supervise ME models, yet their optimization directions are substantial misaligned with the factual ranking ability (AUC). Therefore we propose an end-to-end ranking driven ME paradigm that explicitly optimizes the multi-objective AUC metric:

$$\theta^* = \operatorname{argmax}_{\theta} \mathcal{G}(\theta) \quad (5)$$

## 4 HarmonRank

### 4.1 Alignment to ranking

**4.1.1 Rank-based AUC formulation.** Since  $\mathcal{G}$  is non-differentiable w.r.t.  $\theta$ , existing wisdom usually maximize AUC via surrogate function to approximate pairwise comparing function  $\mathbb{I}(s_i \geq s_j)$  i.e., pairwise logistic [7] and pairwise square [6] functions. However, this formulation brings large inconsistency between physical AUC computation. Meanwhile, pairwise computation introduce quadratic computation cost during training, which hinders further scaling on datasets. To avoid these problems, we resort to alternative formulation for AUC computation.

In this section, we temporarily omit the subscripts  $m$  of objectives for simplicity. When sorting all positive and negative samples in an increasing order, AUC can be simplified to compute the rank sum of positive samples for the good property of ordered list [10]:

$$\mathcal{G}(\mathbf{w}) = \frac{\langle \mathbf{r}, \mathbf{y} \rangle - |\mathcal{D}^+| \cdot (|\mathcal{D}^+| + 1)/2}{|\mathcal{D}^+| \cdot |\mathcal{D}^-|} \quad (6)$$

where the vector  $\mathbf{r} = \text{Rank}(\mathbf{s})$  represents the ranks of all  $N$  samples and  $\mathbf{y}$ . It is noteworthy that, the conventional pairwise formulation suffers from cost inefficiency because of additional computations for positive-negative pairs with reverse orders ( $s_+ < s_-$ ). Under the ordered setting, AUC computation can be simplified to  $O(n \log n)$  time complexity. To optimize  $\mathcal{G}(\mathbf{w})$ , we only need to optimize  $\langle \mathbf{r}, \mathbf{y} \rangle$  for other terms are constant numbers. So the objective can be simplified as:

$$\theta^* = \operatorname{argmax}_{\theta} \langle \mathbf{r}, \mathbf{y} \rangle \quad (7)$$

However, for rank operation  $\text{Rank}(\cdot)$  is non-convex, discontinuous gradients is infeasible for  $\mathbf{s}$ . To alleviate this, we employ a fast differentiable ranking algorithm [2] to enable gradient backpropagation from supervisions to the ensemble model.

**4.1.2 Differentiable Ranking.** Following [2], we cast ranking operation (in increasing order here) as a discrete optimization problem over all feasible permutations  $\Sigma$ .

$$\mathbf{r}^* = \operatorname{argmax}_{\sigma \in \Sigma} \langle \mathbf{s}, \mathbf{r}_\sigma \rangle \quad (8)$$

where  $|\Sigma| = A_N^N$  and we desire the earlier-ranked samples should have smaller values. To transform this discrete optimization form to a continuous optimization problem, this method introduces a convex hull composed of all feasible permutations in  $\Sigma$ , which forms a permutohedron  $\mathcal{P}(\mathbf{r})$ :

$$\mathcal{P}(\mathbf{r}) := \operatorname{conv}(\mathbf{r}_\sigma | \sigma \in \Sigma) \quad (9)$$

To make it a convex objective, this method employs a quadratic regularization into the original optimization problem:

$$P(\mathbf{s}, \mathbf{r}) = \operatorname{argmax}_{\mathbf{t} \in \mathcal{P}(\mathbf{r})} \langle \mathbf{s}, \mathbf{t} \rangle - \frac{1}{2} \|\mathbf{t}\|^2 = \operatorname{argmin}_{\mathbf{t} \in \mathcal{P}(\mathbf{r})} \frac{1}{2} \|\mathbf{t} - \mathbf{s}\|^2 \quad (10)$$

In this way, the original problem has been transformed to the projections to the permutohedron, which is a strong convex function. This approach enables forward propagation with  $O(n \log n)$  time complexity for sorting operation. In the same time, it cost only  $O(n)$  time complexity during backward propagation for the gradients computation can be finished in the sorted sequence [2].

### 4.2 Alignment among objectives

We find prior wisdom consistently overlook the alignment between multiple objectives, which makes model hard to learn the shared ranking abilities among objectives. As shown in Fig. 4, different objectives can be partially aligned with varying degrees. To fill this gap, we design a dual-path architecture to integrate multiple scores in both *one-step* (relation-agnostic) manner and *two-step* (relation-aware) manner between objectives. As shown in Fig. 2

(a), we split our framework into two parallel components: relation-aware module and relation-agnostic module. The output scores of two modules are lately fused into a united score to compute the AUC loss.

**4.2.1 Relation-aware Module.** We align the shared parts between objectives with a relation-aware two-step paradigm, first *align* then *ensemble*. For *align* step, as shown in Fig. 2(b), we utilize self-attention mechanism [20] to capture pairwise relations between objectives. Through dynamic computation of relations between objectives, the aligned common parts between them are extracted. Specifically, the softmax normalized dot products between projected objective vectors,  $\mathbf{Q}_r$  and  $\mathbf{K}_r$ , form the self attention matrix  $\mathbf{A}_r \in \mathbb{R}^{m \times m}$  between them. This matrix naturally represents the relation strengths between objectives. Then the original score embeddings are integrated into the representations  $\mathbf{x}_r$  according to the attention matrix.

$$\mathbf{Q}_r, \mathbf{K}_r, \mathbf{V}_r = \mathbf{x} \mathbf{W}^{\mathbf{Q}_r}, \mathbf{x} \mathbf{W}^{\mathbf{K}_r}, \mathbf{x} \mathbf{W}^{\mathbf{V}_r} \quad (11)$$

$$\mathbf{A}_r = \text{Softmax}(\mathbf{Q}_r \mathbf{K}_r^\top / \sqrt{d_k}) \quad (12)$$

$$\mathbf{x}_r = \mathbf{A}_r \mathbf{V}_r \quad (13)$$

Although we achieve inter-objective alignment, we still lack clear guidance on how to fuse multiple objectives into a unified score. Fortunately, user-specific personalized information, including user profile and context feature, can serve as strong inductive bias to guide this fusion. We cast the personalized information as a *query*, and search with it over multi-objective scores. We use the searched result as the fused score encodings to obtain ensemble score. In this way, we implicitly let model answer a question that ‘*Which objects can best represent the user’s holistic intentions in the current context?*’. Specifically, we transform personalized information into the query vector  $\mathbf{Q}_p$  by linear projection, similar to key and value vectors.

$$\mathbf{Q}_p, \mathbf{K}_p, \mathbf{V}_p = \mathbf{P} \mathbf{W}^{\mathbf{Q}_p}, \mathbf{x}_p \mathbf{W}^{\mathbf{K}_p}, \mathbf{x}_p \mathbf{W}^{\mathbf{V}_p} \quad (14)$$

$$\mathbf{A}_p = \text{Softmax}(\mathbf{Q}_p \mathbf{K}_p^\top / \sqrt{d_k}) \quad (15)$$

Then attention weights  $\mathbf{A}_p \in \mathbb{R}^{1 \times m}$ , computed via dot product over all objective vectors  $\mathbf{s}_r$ , can serve as personalized guidance for importance of objectives for ensemble models. Then we fused score encodings by attention weights and transform the output to scalar ensemble score  $\mathbf{s}_1 \in \mathbb{R}$  by a linear projection layer.

$$\mathbf{s}_1 = \mathbf{w}_1^\top (\mathbf{A}_p \mathbf{V}_p) + b_1 \quad (16)$$

**4.2.2 Relation-agnostic Module.** Although we have effectively align the shared parts between different objectives, we still need to ensure that original information of each objective score can be fully preserved in final ensemble process. To this end, we introduce a relation-agnostic module (see Fig. 2(c)). In this module, we employ a gate mechanism to dynamically adjust the importance of different objectives based on their input scores. We obtain the gating coefficients  $\mathbf{g} \in [0, 1]^m$  by projecting score encodings through a linear layer with sigmoid activations. We control the score-wise retaining ratio of all score encodings through Hadamard product between coefficients and score encodings. We then compute the output ensemble score by a final linear fusion layer over gated

encodings.

$$\mathbf{g} = \text{Sigmoid}(\mathbf{w}_g^\top \mathbf{x} + b_g) \quad (17)$$

$$\mathbf{s}_2 = \mathbf{w}_2^\top (\mathbf{g} \odot \mathbf{x}) + b_2 \quad (18)$$

Simultaneously, to make ensemble model to learn a first-order linear fusion scheme, we maintain a parallel linear fusion pathway. In this way, we prevent model performance degradation when we add previous high-order compositions between objectives and make the whole ensemble model more robust.

$$\mathbf{s}_3 = \mathbf{w}_3^\top \mathbf{x} + b_3 \quad (19)$$

Finally, we obtain the output ensemble score by additive fusion of the outputs of both relation-aware module ( $\mathbf{s}_1$ ) and relation agnostic module ( $\mathbf{s}_2$  and  $\mathbf{s}_3$ ).

$$\mathbf{s} = \mathbf{s}_1 + \mathbf{s}_2 + \mathbf{s}_3 \quad (20)$$

### 4.3 Pre-processing

Before feed the score into relation-aware and relation-agnostic modules. We apply discretization embedding to represent the multi-objective scores to obtain non-linear representation. We use a simple equal distance discretization embedding technique to transform scalar scores to embeddings [8].

$$\mathbf{e}^m = \mathbf{E}^m \cdot \text{floor}(\frac{\mathbf{s}^m}{B}) \quad (21)$$

where  $B$  is the number of discrete buckets and  $\mathbf{E}^m$  is the embedding matrix for the  $m$ th objective. The final inputs for the ranking model is the concatenation of both these discrete embeddings:  $\mathbf{x} = [\mathbf{e}^1; \dots; \mathbf{e}^m]$ . In this way, we empower the model more non-linear fitting power comparing to simply using the scalar score representations.

## 5 Experiments

In this section, we conduct extensive online and offline experiments to verify the efficacy of our model following 4 research questions:

- **RQ1:** How does our model perform on industrial recommendation datasets?
- **RQ2:** How our module design and hyperparameter choice impact the performance?
- **RQ3:** Can our method bring improvements of A/B test metrics on online product environment?
- **RQ4:** How our method impact trade-off between objectives? What do the model learn in multiple objective alignment?

### 5.1 Implementation Details

Before training ensemble model, we firstly prepare the input multi-objective scores via performing inference with a high-capacity ranking model over both datasets. For Kuaishou-Elive, we use the online in-service model trained incrementally by years of logs. For the public TenRec dataset, we train a standard MMOE [13] ranking model. Based on prepared multi-objective scores, all offline models are trained with 500 epochs with SGD optimizer. In terms of online training model with streaming data, it is usually trained for one epoch for the consideration of run-time cost and one-epoch overfitting risk in ranking stage. This scheme results in low sample efficiency. Since the model of ME stage is much more lightweight than MP stage and no sparse ID feature is used (cause of one-epoch

method	TenRec-QKVideo		Kuaishou-ELive	
	3-objectives	5-objectives	3-objectives	5-objectives
Multi-objective BCE [3]	2.2420	3.6465	2.1555	3.6682
Label aggregation [11]	2.4040	3.8311	2.0765	3.6883
Reinforce learning [16]	2.2488	3.9074	2.1930	3.7467
Ours	<b>2.4617</b>	<b>3.9186</b>	<b>2.2191</b>	<b>3.7522</b>

**Table 1: Offline results on AUC sum on two industrial datasets under two settings. For TenRec-QKVideo, ‘3 objectives’ are *click*, *like* and *follow*, while ‘5 objectives’ include *click*, *like*, *follow*, *share* and *long view*. For Kuaishou-ELive, the ‘3 objectives’ are *buy*, *follow* and *long view*, while ‘5 objectives’ include *buy*, *follow*, *like*, *comment* and *long view*.**

overfitting), we train 20 epochs for each batch of streaming samples, to balance run-time cost and sample efficiency. We set learning rate to  $1e-4$  and batch size = 10240 for all methods.

## 5.2 Datasets

To evaluate the performance of our method and compared baselines, we conduct comprehensive experiments on two real-world industrial datasets.

Since there are few public live-streaming e-commerce dataset, we build a new dataset called *Kuaishou E-Live*, which contains both e-commerce feedback (purchase) and user engagement oriented feedbacks (long view, like, follow and comment). We built it by sampling millions of exposure logs at Kuaishou e-commerce platform, which is a pioneering live-streaming e-commerce platform with over 400 million DAUs. We utilize several context and user profile features including the hour of a day, app version, age and gender, *etc.*, to characterize user preference in ensemble learning.

Moreover, to verify the universality of our method, we conduct experiments on a public short video recommendation dataset, TecRec-QKVideo [23]. TecRec-QKVideo is collected from QQ-KAN video feeds platforms. It contains over 1M user interaction logs including five type of feedbacks, click, like, share, follow and long view. For the need of personalized ensemble, we utilize several user profile features like age, gender, *etc*. We train our method and compared methods with the same equal loss weights (all weights set to 1.0) for fair comparison on objective trade-offs. We refer more details about dataset to appendix section A.

## 5.3 Compared Methods.

We compare our methods with most representative methods on multi-objective ensemble task. For fair comparison, we use the same network structure as HarmonRank on these baselines.

- **Multi-objective binary cross entropy based (M-BCE)** [3]: This method enables optimization towards multiple objectives by integrating joint learning under multiple independent binary cross entropy losses for different objectives.
- **Reinforce learning (RL) based** [16] : RL-based method formulates multi-objective ensemble as a Markov decision process, and treats input multi-objective scores as the ‘state’ and the multi-objective fusion score as the ‘action’. The multi-objective AUC over a batch of data serves as ‘reward’.
- **Label aggregation based** [4, 11] : Label aggregation based method transforms multi-objective learning into single-objective learning by fusing multiple binary labels to a unified regression label. Then it utilizes mean square error loss between the ensemble score and the aggregated label to optimize the ensemble model.

## 5.4 Offline Results (RQ1)

We evaluate the efficacy of our model by the multi-objective AUC sum. We present the results on two settings, *i.e.*, 3 objectives and all 5 objectives, to verify the conclusion consistency over different settings. For TenRec-QKVideo, ‘3 objectives’ are *click*, *like* and *follow*, while ‘5 objectives’ include *click*, *like*, *follow*, *share* and *long view*. For Kuaishou-ELive, the ‘3 objectives’ are *buy*, *follow* and *long view*, while ‘5 objectives’ include *buy*, *follow*, *like*, *comment* and *long view*.

The experimental results on two datasets are shown in Tab. 1. On the TenRec-QKVideo dataset, our proposed method outperforms MBCE [3] by 27.2 pp (**3.919** v.s. 3.647) for 5-objective AUC sum. On the Kuaishou-ELive dataset, our model outperforms MBCE by 8.4 pp (**3.7522** v.s. 3.6682) for 5-objective AUC sum. The comparison results to the MBCE model demonstrate the efficacy of our proposed ranking-aligned ensemble model.

The RL-based model is the best performing baseline on both datasets. On the TenRec-QKVideo dataset, our model outperforms RL-based model [16] by 1.2 pp (**3.919** v.s. 3.907) for 5-objective AUC sum. On the Kuaishou-ELive dataset, our model outperforms RL-based model by 0.55 pp (**3.7522** v.s. 3.7467). These results verify our continuous gradient-based method is superior to RL policy gradient based methods. In a nutshell, our model consistently outperforms the best-performing baselines on both two datasets in a large margin in terms of different experimental settings.

## 5.5 Ablation study (RQ2)

We conduct comprehensive ablation study on Kuaishou-ELive dataset to investigate the impact of different AUC optimization losses and different model structures.

5.5.1 *Different AUC optimization losses.* Other than our proposed differentiable ranking-based AUC maximization method, we compare several popular pairwise AUC surrogate losses *i.e.*, pairwise logistic [7], pairwise square [6] and the state-of-the-art instance-wise AUC maximization method AUCM [24]. Pairwise methods maximize AUC objective with logistic or square function surrogate to approximate pairwise  $\mathbb{I}(f(\mathbf{x}_+) \geq f(\mathbf{x}_-))$ . For pairwise computation nature, these methods perform a  $O(n^2)$  time complexity during training process. Different from them, AUCM transforms pairwise maximization objective to an equivalent instance-wise min-max problem, which reduces the training time complexity to  $O(n)$ . Notwithstanding these efforts, the inherent inconsistency with the AUC metric persists. As shown in Tab. 2, our proposed differentiable ranking-based method consistently outperforms other AUC losses. This is because our method eliminates the need of

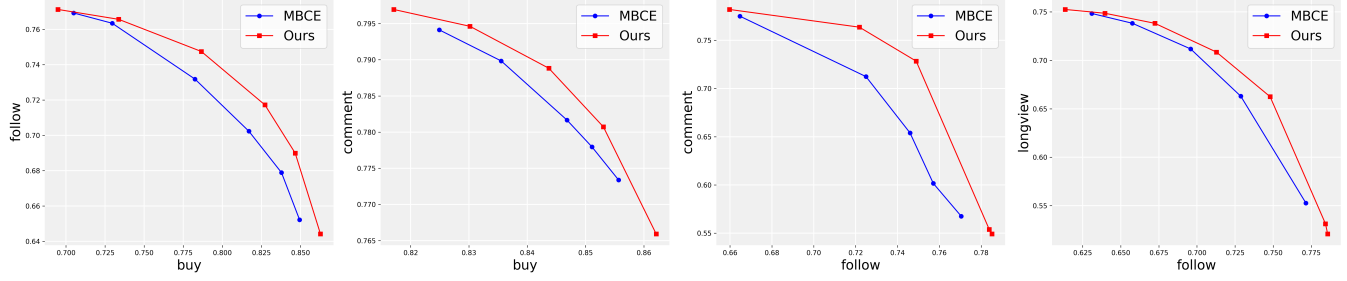


Figure 3: The tradeoff curves between competing objectives of the different models on the Kuaishou Elive dataset.

Different Losses	AUC Sum	Time-complexity
Pairwise Square	3.7415	$O(n^2)$
Pairwise Logistic	3.7433	$O(n^2)$
AUCM	3.7412	$O(n)$
Ours (Differentiable Ranking)	<b>3.7522</b>	$O(n \log n)$

Table 2: Results on Kuaishou-ELive for different AUC-driven losses.

defining surrogate functions which makes it inevitably misaligned with AUC metric. This experiment fundamentally demonstrates the superiority of our method over existing methods.

**5.5.2 Model components.** As shown in Tab. 3, we conducted a comprehensive ablation study to evaluate the impact of different modules in our proposed method. We conduct three ablations in the relation aware module. First, when removing the self-attention-based alignment module (Ours w/o Self-Attention), we find the corresponding variant exhibits a 0.3pp drop in AUC sum (3.7494 v.s. **3.7522**), indicating the indispensable role of relation modelling between different objective score encodings. Second, the variant without personalized feature (Ours w/o Personalized Feat.) exhibits a 0.6pp performance degradation (3.7464 v.s. **3.7522**), demonstrating their significant contribution in guiding score importance weighting. Third, in terms of the manner of introducing personalized information, in addition to cross-attention mechanism, we experiment with an alternative baseline that simply concatenating personalized features with self-attention outputs before linear projection (Ours w/o Cross-Attention). Our method outperforms this baseline by 0.1pp in AUC sum (**3.7522** v.s. 3.5712). We attribute this to linear projection’s inability to facilitate dense interactions between personalized features and score encodings which can be fulfilled by cross-attention’s dynamic weighting mechanism.

In relation-agnostic module, we conduct ablations on two sub-components inside it. First, we try to remove the gate mechanism (Ours w/o Gate Mechanism), which leads to substantial performance drop (1.6pp), confirming its critical function for denoising and importance score selection. In addition, the variant without linear fusion pathway Ours w/o Linear results in a 0.3pp AUC sum decrease (3.7493 v.s. **3.7522**), suggesting that the first-order linear fusion can effectively enhance model robustness.

**5.5.3 Pre-processing.** We also conduct experiments on different choices of number of buckets for score discretization. As shown in Tab. 4, we find the variant without discretization (No Disc.) results into a significant performance decrease (3.7522 → 3.7470),

Method	AUC Sum
<i>In relation-aware module</i>	
Ours w/o Self-Attention	3.7494
Ours w/o Personalized Feat.	3.7464
Ours w/o Cross-Attention	3.7512
<i>In relation-agnostic module</i>	
Ours w/o Gate Mechanism	3.7362
Ours w/o LinearPath	3.7493
<b>Ours</b>	<b>3.7522</b>

Table 3: Results on Kuaishou-Elive for different variants of our proposed structure with different components removed.

#DiscretizationBuckets	AUC Sum
No disc.	3.7470
100	3.7507
300	<b>3.7522</b>
600	3.7492

Table 4: Results on Kuaishou-Elive for different number of discretization buckets.

which demonstrates the necessity of discretization. We find different number of buckets present different performance, this may be because excessively fine-grained discretization approach the no-discretization situation, whereas overly coarse discretization make it lack discrimination between high and low scores. An appropriately number of buckets, i.e., 300 here, yields optimal performance.

## 5.6 Online Results (RQ3)

We deploy our method in the production environment of Kuaishou e-commerce live-streaming platform to conduct online A/B testing for 5 days. It is noteworthy that the online base model is MBCE. Compared with the base model. As shown in Tab. 5 our model achieves significant improvements across all objectives, e.g., 2.635% on core purchases metric and 0.451% on follow metrics, which verify the effectiveness of our proposed HarmonRank for offline-online consistent improvements.

## 5.7 Analysis (RQ4)

**5.7.1 Impact on Pareto frontier.** To validate whether our method can achieve Pareto improvement (i.e., improving at least one objective without deteriorating others) in multi-objective optimization,

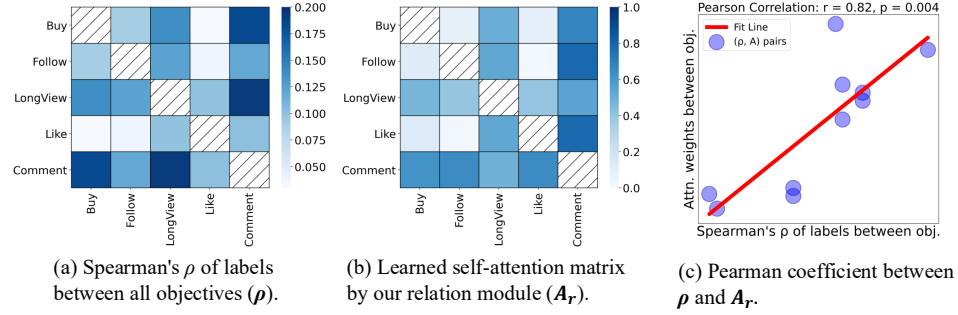


**Figure 4: Consistency analysis between the learned attention matrix  $A_r$  and ground-truth data distribution (label's Spearman Rank Correlation  $\rho$ ).**

Objectives	Gain
Purchase	+2.635%
Comment	+3.034%
Follow	+0.451%
Watch time	+0.290%
Like	+1.673%

**Table 5: Online A/B Test Performance.**

we compare the Pareto frontiers between our proposed method and Multi-objective BCE. Given that the loss weights assigned to different objectives significantly influence their corresponding AUC performance, we systematically adjusted the allocation of loss weights to obtain a series of AUC values under various trade-off scenarios. As seen in Fig. 3, our method consistently achieves superior trade-off curves over Multi-objective BCE (MBCE). Taking *buy* and *follow* objectives as examples, our method outperforms MBCE in terms of AUC for both objectives across all weight allocations. The similar phenomenon can be observed in trade-off curves between other objective pairs, including *comment v.s. buy*, *comment v.s. follow* and *long view v.s. follow* in Fig. 3.

**5.7.2 Inter-objective alignment analysis.** To shed light on the factual degree of alignment between objectives (ground-truth), and which of them can be learned in inter-objective alignment modules (predicted), we visualize inter-objective correlations in two ways. For the ground-truth relations, we compute Spearman's rank correlation coefficients  $\rho$  between different objectives over the labels, which measures the monotonic alignment between the ranks of two objective labels. For predicted relations, we visualize the attention weights inferred by our method's relation module.

$$\rho_{mn} = \text{Spearmanr}(\mathbf{y}_m, \mathbf{y}_n) \quad (22)$$

$$\mathbf{A}_r^{mn} = \mathbf{A}_r[m, n] \quad (23)$$

As shown in the Fig. 5, we present the  $\rho_{buy,:}$  and  $\mathbf{A}_r^{buy,:}$  between *buy* objective and all other objectives. It can be observed that the learned attention matrix exhibits strong alignment with label ranking, showing consistent patterns: *comment > long view > follow > like*. This demonstrates that our inter-objective alignment module effectively captures latent dependencies. The particularly strong correlations of *buy v.s. long view* and *buy v.s. comment* are because the users with immediate purchase willingness tend to engage in

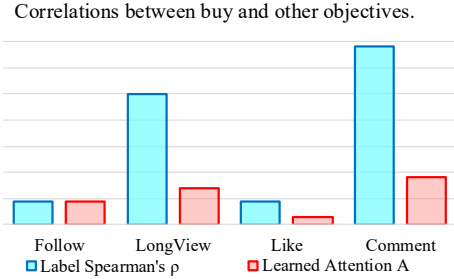


**Figure 5: Two views of the correlations between *buy* objective and other objectives: Spearman's rank correlation ( $\rho$ ) of labels and learned attention matrix  $A_r$ .**  
prolonged viewing for product explanations and active questioning via comments.

Moreover, to quantitatively validate the consistency between learned patterns in the attention matrix and ground-truth inter-objective alignment, we try to compute the correlation strength between the ground-truth and predicted relations. To preserve more absolute correlation scales in attention matrix, we apply sigmoid instead of softmax normalization over the original dot product matrix. We compute the correlation between label Spearman's  $\rho$  and predicted attention matrix  $A_r$ .

$$r = \text{Pearson}(\rho, \mathbf{A}_r) \quad (24)$$

Results in Fig. 4 demonstrate remarkable consistency ( $r = 0.82, p = 0.004$ ) between learned attentions and empirical alignment, confirming our method's capability to accurately capture inter-objective alignment by our two-step ensemble paradigm.

## 6 Conclusion

The proposed HarmonRank framework addresses two limitations in multi-objective ensemble problem in recommendation systems. For the lack of alignment to ranking, we formulate AUC computation as rank-sum problem and use differentiable ranking to enable end-to-end AUC optimization. For the lack of alignment between different objectives, we propose a two-step paradigm, first *align* then *ensemble*. This paradigm effectively align the shared parts between objectives. Extensive online and offline experimental results demonstrate significant improvements of our proposed HarmonRank over existing methods.

## References

- [1] Donald Bamber. 1975. The area above the ordinal dominance graph and the area below the receiver operating characteristic graph. *Journal of mathematical psychology* 12, 4 (1975), 387–415.
- [2] Mathieu Blondel, Olivier Teboul, Quentin Berthet, and Josip Djolonga. 2020. Fast differentiable sorting and ranking. In *International Conference on Machine Learning*. PMLR, 950–959.
- [3] Jiangxia Cao, Pengbo Xu, Yin Cheng, Kaiwei Guo, Jian Tang, Shijun Wang, Dewei Leng, Shuang Yang, Zhaojie Liu, Yanan Niu, et al. 2025. Pantheon: Personalized Multi-objective Ensemble Sort via Iterative Pareto Policy Optimization. *arXiv preprint arXiv:2505.13894* (2025).
- [4] David Carmel, Elad Haramaty, Arnon Lazerson, and Liane Lewin-Eytan. 2020. Multi-objective ranking optimization for product search using stochastic label aggregation. In *Proceedings of The Web Conference 2020*. 373–383.
- [5] Wei Cheng, Yucheng Lu, Boyang Xia, Jiangxia Cao, Kuan Xu, Mingxing Wen, Wei Jiang, Jiaming Zhang, Zhaojie Liu, Liyin Hong, et al. 2025. ChorusCVR: Chorus Supervision for Entire Space Post-Click Conversion Rate Modeling. *arXiv preprint arXiv:2502.08277* (2025).
- [6] Wei Gao, Rong Jin, Shenghuo Zhu, and Zhi-Hua Zhou. 2013. One-pass AUC optimization. In *International conference on machine learning*. PMLR, 906–914.
- [7] Wei Gao and Zhi-Hua Zhou. 2012. On the consistency of AUC pairwise optimization. *arXiv preprint arXiv:1208.0645* (2012).
- [8] Huirong Guo, Bo Chen, Ruiming Tang, Weinan Zhang, Zhenguo Li, and Xiuqiang He. 2021. An embedding learning framework for numerical features in ctr prediction. In *Proceedings of the 27th ACM SIGKDD Conference on Knowledge Discovery & Data Mining*. 2910–2918.
- [9] James A Hanley and Barbara J McNeil. 1982. The meaning and use of the area under a receiver operating characteristic (ROC) curve. *Radiology* 143, 1 (1982), 29–36.
- [10] James A Hanley and Barbara J McNeil. 1982. The meaning and use of the area under a receiver operating characteristic (ROC) curve. *Radiology* 143, 1 (1982), 29–36.
- [11] Jiayu Li, Peijie Sun, Zhefan Wang, Weizhi Ma, Yangkun Li, Min Zhang, Zhoutian Feng, and Daiyue Xue. 2023. Intent-aware ranking ensemble for personalized recommendation. In *Proceedings of the 46th international ACM SIGIR conference on research and development in information retrieval*. 1004–1013.
- [12] Xiao Lin, Hongjie Chen, Changhua Pei, Fei Sun, Xuanji Xiao, Hanxiao Sun, Yongfeng Zhang, Wenwu Ou, and Peng Jiang. 2019. A pareto-efficient algorithm for multiple objective optimization in e-commerce recommendation. In *Proceedings of the 13th ACM Conference on recommender systems*. 20–28.
- [13] Jiaqi Ma, Zhe Zhao, Xinyang Yi, Jilin Chen, Lichan Hong, and Ed H Chi. 2018. Modeling task relationships in multi-task learning with multi-gate mixture-of-experts. In *Proceedings of the 24th ACM SIGKDD international conference on knowledge discovery & data mining*. 1930–1939.
- [14] Xiao Ma, Liqin Zhao, Guan Huang, Zhi Wang, Zelin Hu, Xiaoqiang Zhu, and Kun Gai. 2018. Entire space multi-task model: An effective approach for estimating post-click conversion rate. In *The 41st International ACM SIGIR Conference on Research & Development in Information Retrieval*. 1137–1140.
- [15] Jonas Močkus. 1974. On Bayesian methods for seeking the extremum. In *IFIP Technical Conference on Optimization Techniques*. Springer, 400–404.
- [16] Changhua Pei, Xinru Yang, Qing Cui, Xiao Lin, Fei Sun, Peng Jiang, Wenwu Ou, and Yongfeng Zhang. 2019. Value-aware recommendation based on reinforcement profit maximization. In *The World Wide Web Conference*. 3123–3129.
- [17] Reuven Y Rubinstein and Dirk P Kroese. 2004. *The cross-entropy method: a unified approach to combinatorial optimization, Monte-Carlo simulation and machine learning*. Springer Science & Business Media.
- [18] Hongyan Tang, Junning Liu, Ming Zhao, and Xudong Gong. 2020. Progressive layered extraction (ple): A novel multi-task learning (mtl) model for personalized recommendations. In *Proceedings of the 14th ACM conference on recommender systems*. 269–278.
- [19] Shuang Tang, Fangyuan Luo, and Jun Wu. 2022. Smooth-auc: Smoothing the path towards rank-based ctr prediction. In *Proceedings of the 45th international ACM SIGIR conference on research and development in information retrieval*. 2400–2404.
- [20] Ashish Vaswani, Noam Shazeer, Niki Parmar, Jakob Uszkoreit, Llion Jones, Aidan N Gomez, Łukasz Kaiser, and Illia Polosukhin. 2017. Attention is all you need. *Advances in neural information processing systems* 30 (2017).
- [21] Yiming Ying, Longyin Wen, and Siwei Lyu. 2016. Stochastic online AUC maximization. *Advances in neural information processing systems* 29 (2016).
- [22] Wenhui Yu, Bingqi Liu, Bin Xia, Xiaoxiao Xu, Ying Chen, Yongchang Li, and Lantao Hu. 2024. Unsupervised Ranking Ensemble Model for Recommendation. In *Proceedings of the 30th ACM SIGKDD Conference on Knowledge Discovery and Data Mining* (Barcelona, Spain) (KDD '24). Association for Computing Machinery, New York, NY, USA, 6181–6189. doi:10.1145/3637528.3671598
- [23] Guanghu Yuan, Fajie Yuan, Yudong Li, Beibei Kong, Shujie Li, Lei Chen, Min Yang, Chenyun Yu, Bo Hu, Zang Li, et al. 2022. Tenrec: A large-scale multipurpose benchmark dataset for recommender systems. *Advances in Neural Information Processing Systems* 35 (2022), 11480–11493.
- [24] Zhuoning Yuan, Yan Yan, Milan Sonka, and Tianbao Yang. 2021. Large-scale robust deep auc maximization: A new surrogate loss and empirical studies on medical image classification. In *Proceedings of the IEEE/CVF International Conference on Computer Vision*. 3040–3049.

## Appendix

In this appendix, we provide more implementation details and experimental results of our proposed HarmonRank. Accordingly, we organize the appendix as follows.

- In Section A, we present more implementation details for our method.
- In Section B, we present practical training speed our method and compared methods.
- In Section C, we test the robustness of different methods under label skew situations.

### A Implementation details

For Kuaishou E-Live, we collect 2M samples by down-sampling from 1-week logs, 1M for training, 0.5M for validation and test set, individually. For TenRec dataset, we collect 2M samples by down-sampling from QK-video dataset.

### B Practical training speed

As shown in Tab. 6, we compare the training speed among different AUC end-to-end losses. The training batch size is set to 10240 for all methods. The ranks of actual training speeds across different methods aligns with their theoretical computational complexity. Due to the pairwise nature of 'PL' (Pairwise Logistic), it exhibits the slowest training speed, while AUCM and MBCE methods achieve the fastest training owing to their instance-wise loss computation with  $O(n)$  complexity. Although our method's training speed lies between pairwise and instance-wise approaches, it delivers the best AUC performance across all methods.

Method	Practical training speed	Theoretical time complexity	AUC Sum
MBCE	27.4K/s	$O(n)$	3.6682
PL	24.8K/s	$O(n^2)$	3.7433
AUCM	26.9K/s	$O(n)$	3.7412
HarmonRank	26.0K/s	$O(n \log n)$	3.7522

Table 6: Comparison of practical training speed.

### C Robustness

To validate the robustness of our method against label skew, we conducted extensive experiments on the Kuaishou E-live dataset. Among our five objectives, the *buy* objective exhibits the most severe label skew with a positive-to-negative ratio of  $1 : 10^3$ . To explore the performance of different methods under harder situations, we artificially strengthen the imbalance of *buy* objective by down-sampling positive samples to ratios of  $1 : 10^4$  and  $1 : 10^5$  respectively on training set only, remaining the test set unchanged.

As shown in the Tab. 7, when facing increasingly severe label skew, all methods exhibit expected AUC degradation. Nevertheless, our HarmonRank consistently maintains superior performance across all scenarios. Crucially, the performance drop of our method (-0.3%) is significantly smaller than those of MBCE and PL (9.8% and 4.3%), demonstrating our methods has exceptional robustness to label distribution skew.

We attribute this phenomenon to different degrees of dependable on negative samples of these methods. As positive samples become sparser, classifying negative samples becomes increasingly trivial, resulting in diminishing gradients from the overwhelming majority of easy negative examples. Consequently, methods like MBCE and PL that heavily rely on negative samples suffer significant performance degradation. In contrast, HarmonRank inherently rely less on negative samples for its rank-sum formulation, whose loss only computes ranks of positive samples and negative samples are utilized only during the differentiable ranking phase.

Methods	Original ( $1 : 10^3$ )	$10 \times$ Skew ( $1 : 10^4$ )	$100 \times$ Skew ( $1 : 10^5$ )
MBCE	3.67	3.48 (-5.2%↓)	3.31 (-9.8%↓)
PL	3.74	3.60 (-3.7%↓)	3.58 (-4.3%↓)
HarmonRank	<b>3.75</b>	<b>3.74 (-0.3%↓)</b>	<b>3.70 (-1.3%↓)</b>

Table 7: Robustness against label skew.